IOP Conference Series: Materials Science and Engineering

PAPER • OPEN ACCESS

Prediction of Indoor Airflow and Contaminant Transport in Office with Coupled Displacement Ventilation and Ceiling Radiant Cooling Panel

To cite this article: Mays Ahyab Shoky *et al* 2021 *IOP Conf. Ser.: Mater. Sci. Eng.* **1094** 012117

Prediction of Indoor Airflow and Contaminant Transport in Office with Coupled Displacement Ventilation and Ceiling Radiant Cooling Panel

Mays Ahyab Shoky, Ali Lafta and Hasanen M Hussein

Mechanical Eng. Dept., University of Technology, Baghdad, Iraq

E-mail: 20046@uotechnology.edu.iq

Abstract. In this research, an experimental and numerical analysis have been conducted to predict the temperature, velocity distribution, and contaminant concentration in indoor spaces conditioned with corrugated ceiling radiant cooling panel (RCP) and Displacement Ventilation. The experiments were done on a model room with dimensions of (1.6m×1.2m×0.8m) built according to a suitable scale factor (1/5) to simulate the temperature, velocity distribution, and CO_2 concentration by 36 measuring devices in an array scheme in three different zones and heights. Two cases were considered in this work, the first was with chilled ceiling panels only (without ventilation) and the second was with displacement ventilation. The experiments primary variable was the mean panel temperature (T_{mp}) with values of (15, 16, and 17°C). The second experimental cases were taken with an air inlet temperature of 24°C and a velocity of 0.7m/s with a range of outdoor air temperatures of (36 to 42°C). A computational fluid dynamics (CFD) program was built up to simulate air distribution in an enclosed environment with the DV-PCB system, which was then validated by the measured data. The validated CFD model was employed to analyze thermal comfort and indoor air quality in the enclosed environment with the DV-PCB coupled system using four indices: vertical temperature gradient, draft rate, normalized contaminant concentration, and age of air. The results indicate that CRCP is quite effective in reducing the temperature gradient created by DV. The results show that there is an enhancement in the total cooling capacity. Most of the computed results were presented as temperature contours and velocity vectors diagrams compared with the experimental work. The comparisons show a reasonably good agreement. Both experimental and numerical studies assist RCP for cooling purposes in the Iraqi climate for its ease, simplicity, and good comfort performance.
Keywords. Radiant cooling, Panels, mixed convection, Environment.

1. Introduction
Panel cooling systems use cold temperature-controlled indoor surfaces on the ceiling to absorb excess thermal energy and remove it from space. In radiant cooling, thermal energy flows from the occupants, equipment, lights, and other surfaces in a room to the actively cooled surface. Temperature is maintained by circulating water through a circuit embedded in or attached to the panel. A temperature-controlled surface is called a radiant panel if 50% or more of the design heat transfer on the temperature-controlled

surface takes place by thermal radiation [1, 2]. The emanating cooling panels (RCP) system uses lengthy radiation into cooled surface to eliminate unwanted temperature from the space and maintains appropriate indoor air quality and tracks indoor air humidity through its air delivery system by providing cool, filtered and dehumidified air. A RCP system distinguishes the role of responsive cooling from those of moisture management and ventilation in its function as air-conditioning systems. Since an RCP system is based on cooled surface radiation for sensitive cooling, it provides comfort at an indoor air temperature higher than an all-air system. RCP systems use water to link the inner radiant surface to an external heat sink as a transportation medium. Water's thermal characteristics permit RCP systems to[3]:

- Extract a certain amount of heat from a building and use less than 25% of transport energy used to remove the same amount of energy from an all-air device, easier to use thermal energy storage systems interface.
- Due to the possibilities of large heat exchange surfaces for RCP systems (the radiant surface typically occupies the larger part of the ceiling or a vertical wall in the room), the panel must have a temperature just a few degrees below the air in the room. This slight temperature differential further decreases the building's energy demand.
- RCP systems reduce dramatically the amount and speed of air transported through buildings only by transporting air required for ventilation purposes, and thereby effectively eliminating drainage. At the same time, as the air does not play a significant cooling function, it must not be cooled well below indoor air temperature [2, 3].

2. Experimental work

The experimental room can be described as an isolated space with well insulated walls. The only connections to the room with the external environment were the supply and return grills and inlet and outlet water headers tubes. An office room was chosen with dimensions (L=8 m, W=6m and H=4m), with (5) occupants. The room needs 0.031 m^3/s (i.e. 2 ACH) as ventilating air according to ASHRAE standard [4]. A Suitable scale factor was assumed to find the model dimensions:

$$l_p/l_m = 5/1 = 5$$

So the model room dimensions were found to be: (L_m=1.6m, Wm=1.2m and H=0.8m).
An aluminum panel (δ=0.5 mm, k=206 W/mK), which is widely used in the Ceiling RCP industry, was considered in this research.
Corrugated RCP was installed on the whole ceiling of the model space. Six parallel copper tubes were attached on the top side of each panel, and insulation material (glass wool) was applied to the top side to prevent heat gains from the plenum space. The tubes used are (5/16”) the outside diameter (Do) and the inside diameter (Di) of the tube are 6.3 and 7.9 mm, respectively [5, 6]. The inside fluid velocity is 0.36 m/s, the spacing between the tubes is 0.13 m, and a header of (1/2”) tube diameter is used with (D_i=11.075 mm and D_o=12.7 mm). So water velocity in the header is ($u_{wp} \approx$ 0.7 m/s) with a pressure drop not to exceed (450 pa/m). The model space walls are made from Perspex. The outdoor air temperature (T_O) range is (36°C to 42°C), and the space temperature (Ta) is maintained at a range of (24°C to 26°C). The air is supplied to the space at neutral temperature of 24 °C through the 0.04m×0.02m side wall grill located on the middle of the wall near the ceiling. The grill discharge air velocity was 0.7m/s according to only ventilation air needed 0.031 m^3/s (2 ACH). All the exterior tubes and connections between test rig and water cooler are well insulated too. Figure (1) shows the schematic diagram for the experimental apparatus. Forty thermocouples type K were used for the temperature measurements. These thermocouples are fixed as follows:

- Two thermocouples were fixed on the inlet and outlet panel tubes to read water temperatures.
- Two thermocouples were fixed on the supply and return grills to the test room to read inlet and outlet air temperatures.

- Thirty-six thermocouples were fixed inside the test room in three levels according to a designed sequence in order to read the air-conditioned space temperatures for human comfort considerations, as shown in Figure (2).

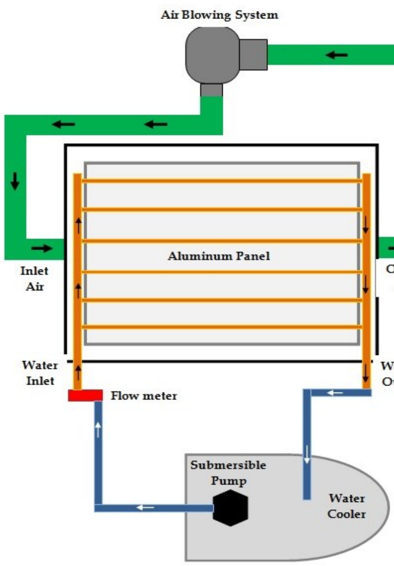

Figure 1. Schematic diagram for the experimental apparatus.

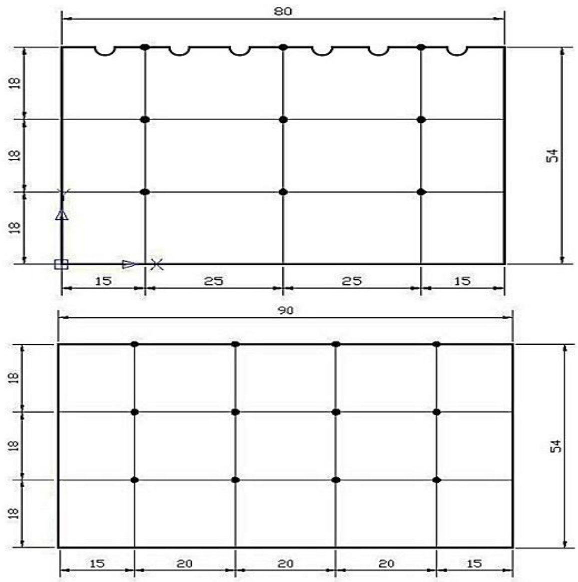

Figure 2. Side and front view for thermocouple arrangement in the model room, dimension in (cm).

3. Basic governing equations

The conservation equations for continuity, momentum, energy and turbulent model can be written as follows [7]. The Conservation of Mass (Continuity) equation:

$$\frac{\partial u}{\partial x}+\frac{\partial v}{\partial y}+\frac{\partial w}{\partial z}=0 \tag{1}$$

And the Navier-Stokes Equations (Momentum) equations are:

$$\frac{\partial(\rho uu)}{\partial x}+\frac{\partial(\rho vu)}{\partial y}+\frac{\partial(\rho wu)}{\partial z}=-\frac{\partial p}{\partial x}+\mu[\frac{\partial^2 u}{\partial x^2}+\frac{\partial^2 u}{\partial y^2}+\frac{\partial^2 u}{\partial z^2}] \tag{2}$$

$$\frac{\partial(\rho uv)}{\partial x}+\frac{\partial(\rho vv)}{\partial y}+\frac{\partial(\rho wv)}{\partial z}=-\frac{\partial p}{\partial y}+\mu\left[\frac{\partial^2 v}{\partial x^2}+\frac{\partial^2 v}{\partial y^2}+\frac{\partial^2 v}{\partial z^2}\right]+S_{bj} \tag{3}$$

$$\frac{\partial(\rho uw)}{\partial x}+\frac{\partial(\rho vw)}{\partial y}+\frac{\partial(\rho ww)}{\partial z}=-\frac{\partial p}{\partial z}+\mu[\frac{\partial^2 w}{\partial x^2}+\frac{\partial^2 w}{\partial y^2}+\frac{\partial^2 w}{\partial z^2}] \tag{4}$$

The energy equation is:

$$\rho\frac{\partial}{\partial x}(uT)+\rho\frac{\partial}{\partial y}(vT)+\rho\frac{\partial}{\partial z}(wT)=\frac{\partial}{\partial x}\left(\Gamma_{eff.h}\frac{\partial T}{\partial x}\right)+\frac{\partial}{\partial y}\left(\Gamma_{eff.h}\frac{\partial T}{\partial y}\right)+\frac{\partial}{\partial z}\left(\Gamma_{eff.h}\frac{\partial T}{\partial z}\right)+S_T \tag{5}$$

where u, v and w are stream-wise, vertical and lateral velocity component respectively, x, y and z are the corresponding directions, and S_{bj} is the buoyancy source or sink term.

The set of governing equation (1) to (5) for the corrugated ceiling RCP cases were solved using FORTRAN 90 with several assumptions, such as steady, incompressible and Newtonian flow. The numerical case setup is achieved with general form of Pressure-Based solver type, absolute velocity formulation and steady state for time consideration. The boundary and initial conditions for the model room are important in obtaining an accurate solution. Momentum, turbulence and thermal boundary conditions for the whole parameters of the model room took place in the numerical work. An acceptable convergence for continuity, momentum and energy equations for laminar flow cases and also K and ε for turbulent flow case was achieved. Average minimum convergences were (1×10^{-4}, 3×10^{-5} and 8×10^{-7}) for continuity, velocities and energy equations respectively, for laminar flow cases and residuals of (5×10^{-4} and 9×10^{-4}) for K and ε respectively added for turbulent flow case (i.e. $u_{a\,i}$=2m/s).

4. Results

Many computational runs were performed at various mean panel temperature, ambient temperature, air inlet temperature and velocity. All results are plotted in one of the planes shown in Figure (3) and Figure (4) which describe the distribution of air velocity in I and K- plane at different inlet velocity and (18℃) inlet air temperature. The numerical temperature vectors are shown in Figures (5) and (6) in I and K-plane at different inlet air velocities and inlet air temperatures (18 ℃). Figure (7) shows the relationship between the temperature of the room with time at inlet air temperatures (18℃) and different-inlet air velocity in a displacement ventilation system. The relationship between the height of the room with co2 concentration inlet air temperatures (18℃) and different-inlet air velocity in a displacement ventilation system is shown in Figure (8). Experimental temperature contours were presented and drawn using TECPLOT program.
The experimental FC heat transfer coefficient is determined by using the simplified correlations estimated by Jeong and Mumma [8]. Experimental enhanced cooling capacity of a corrugated ceiling RCP by FC will be estimated with the simplified model by Jeong and Mumma [9]. Figure (9) shows the distribution of air velocity in I-plane at different inlet velocity and inlet air temperature (18 ℃) with DV /CC and in K-plane as shown in Figure (10). Figure (11) shows the relationship between the temperature of the room with time and Figure (12) between the height of the room with co_2 concentration and both of them at inlet air temperatures (18℃) and different-inlet air velocity in displacement ventilation and cooling ceiling.

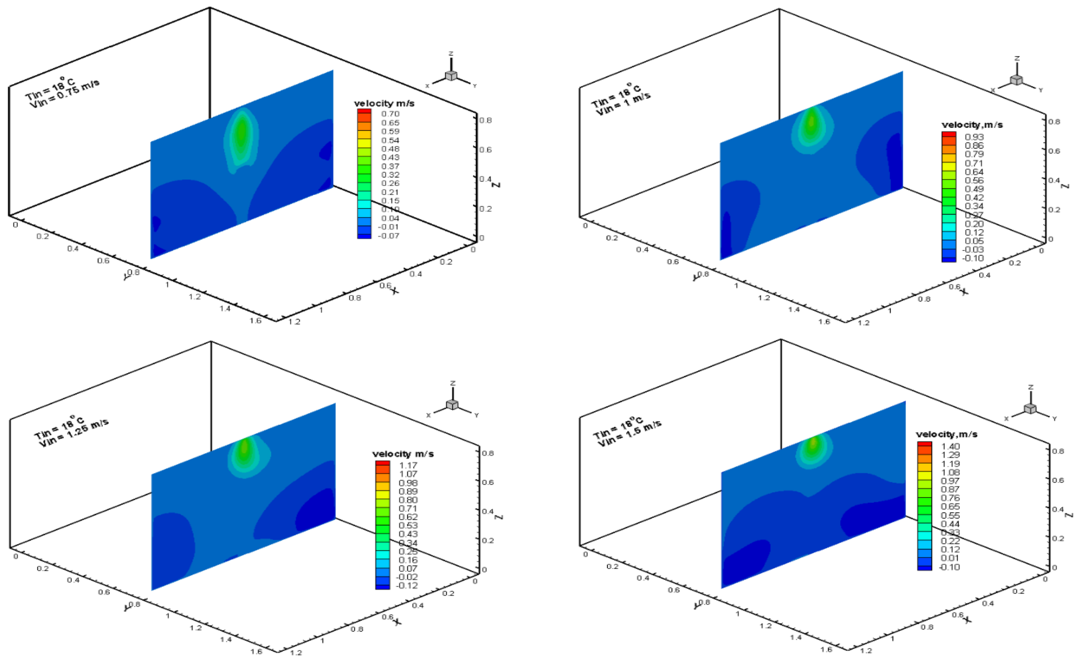

Figure 3. Distribution of air velocity in I-plane at different inlet velocities and inlet air temperature (18^0C) with DV.

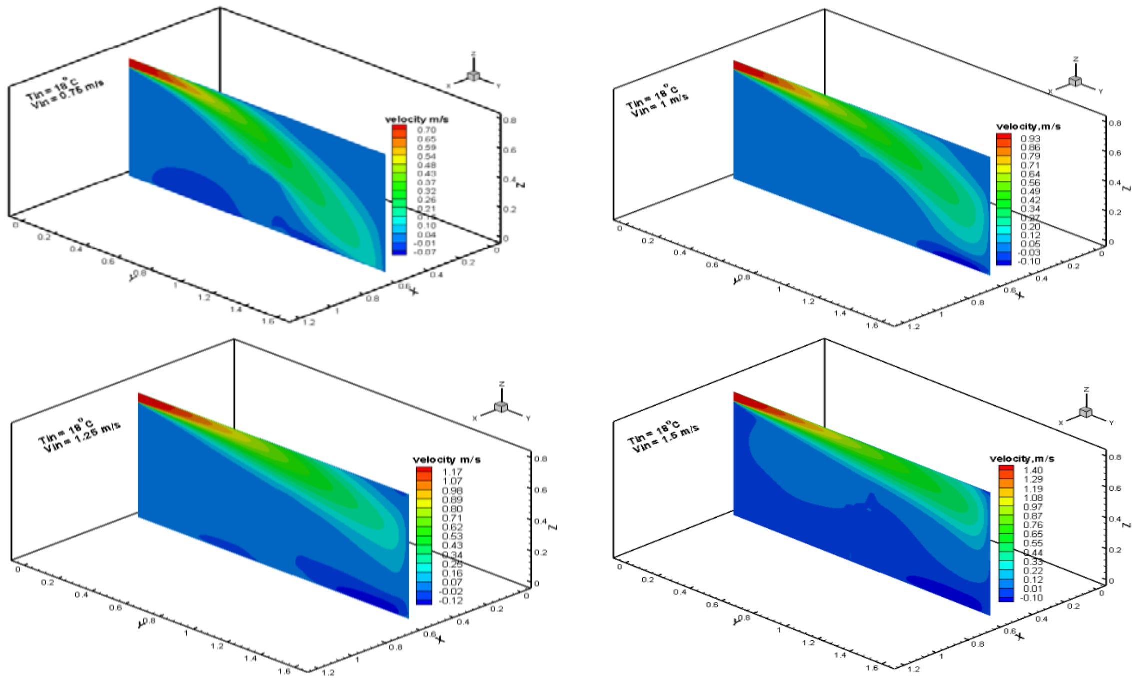

Figure 4. Distribution of air velocity in K-plane at different inlet velocity and inlet air temperature (18^0C) with DV.

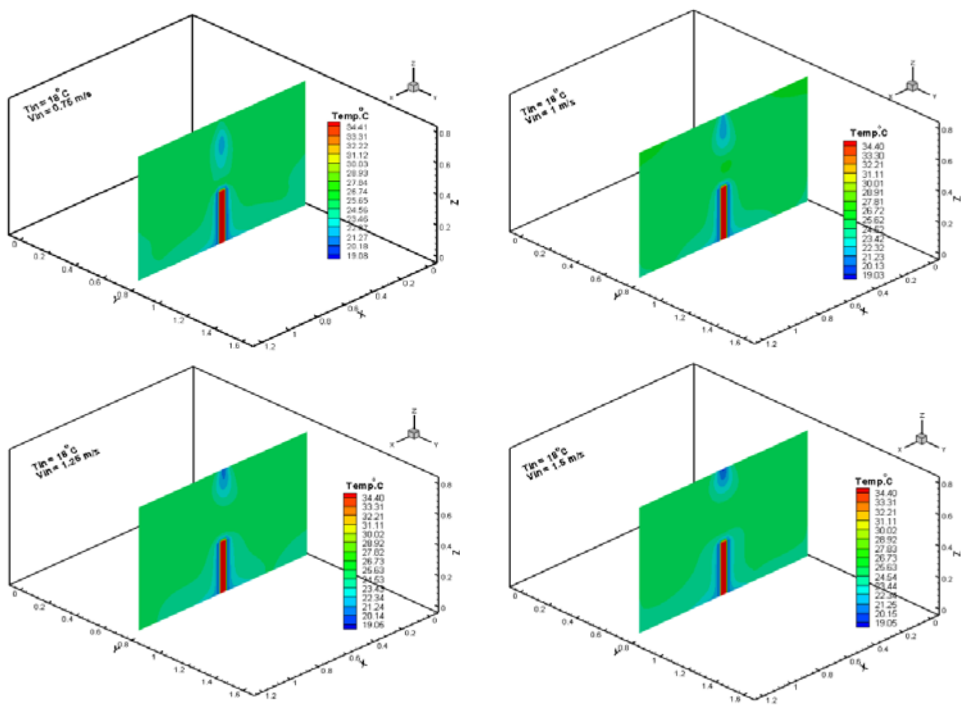

Figure 5. Distribution of air Temperature in K-plane at different inlet velocity and inlet air temperature (18^0C) with DV.

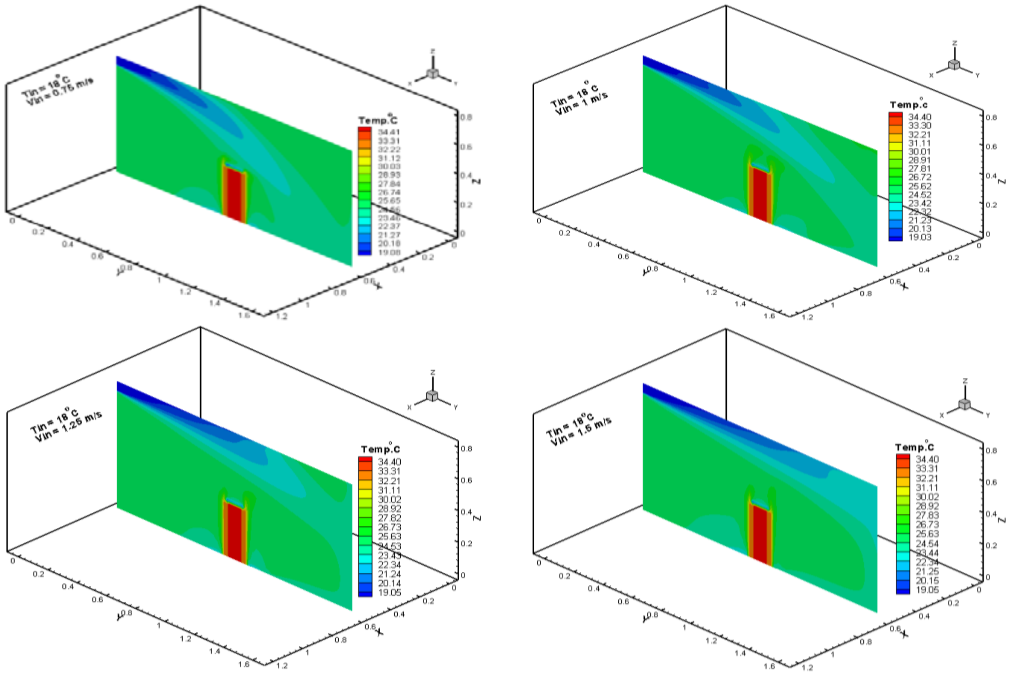

Figure 6. Distribution of air Temperature in K-plane at inlet velocity (0.75 m/s) and inlet air temperature (18^0C) with DV.

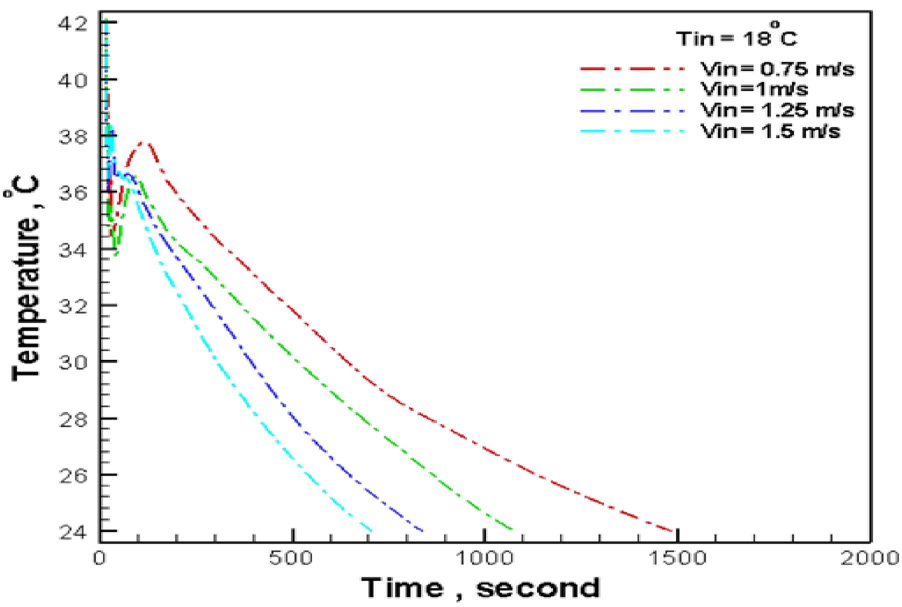

Figure 7. The relationship between the temperatures of the room with time at inlet air temperatures (18 ^{o}C) and different-inlet air velocity in a displacement ventilation system.

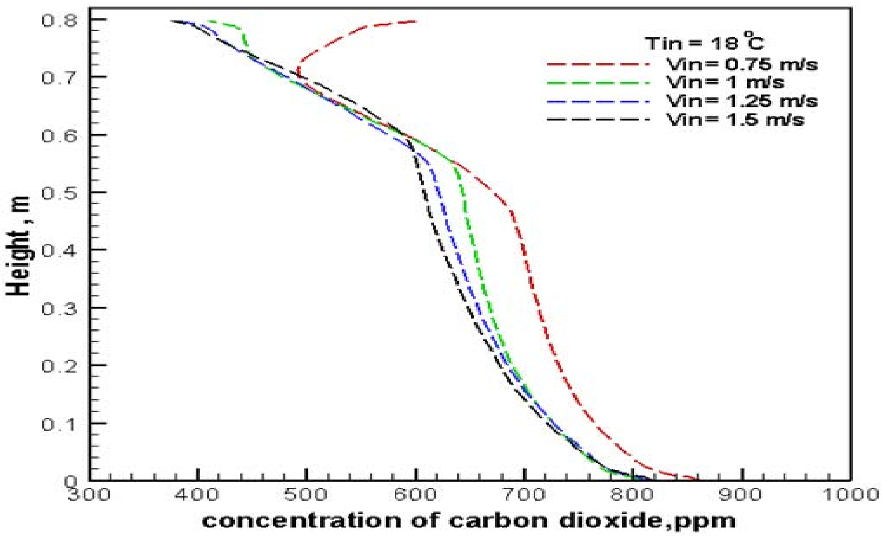

Figure 8. The relationship between the height of the room with Co_2 concentration inlet air temperatures (18 °C) and different-inlet air velocity in a displacement ventilation system.

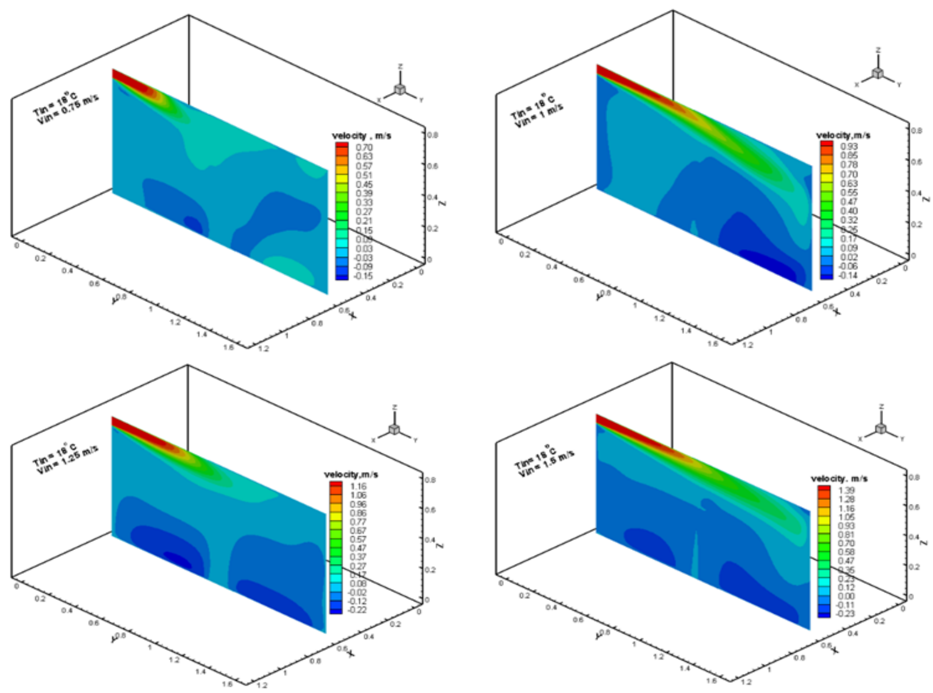

Figure 9. Distribution of air velocity in K-plane at inlet velocity (0.75 m/s) and inlet air temperature (18^0C) with DV /CC.

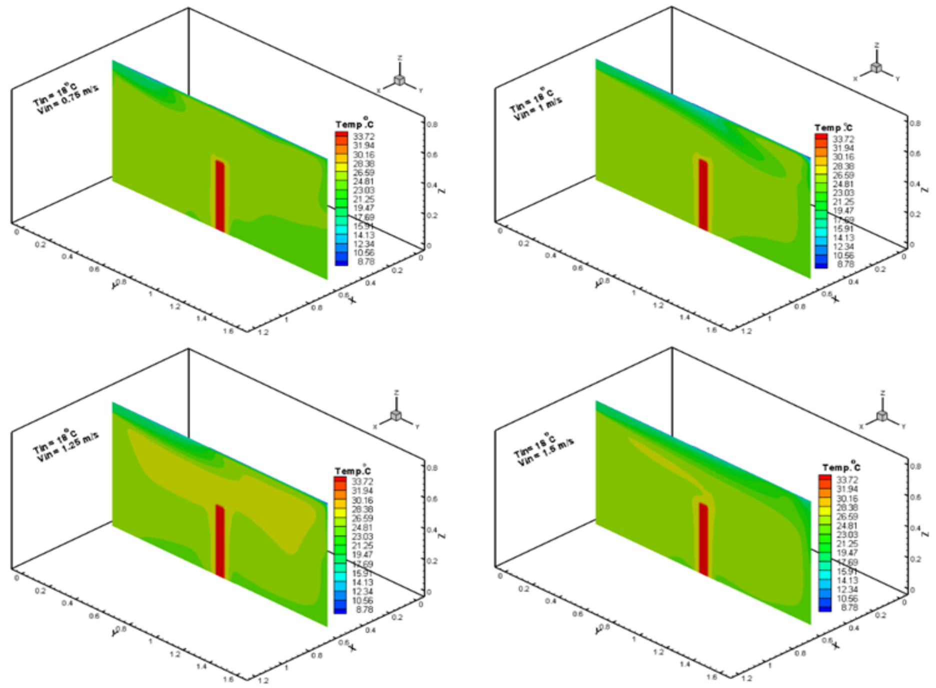

Figure 10. Distribution of air temperature in K-plane at inlet velocity (0.75 m/s) and inlet air temperature (18^0C) with DV/CC.

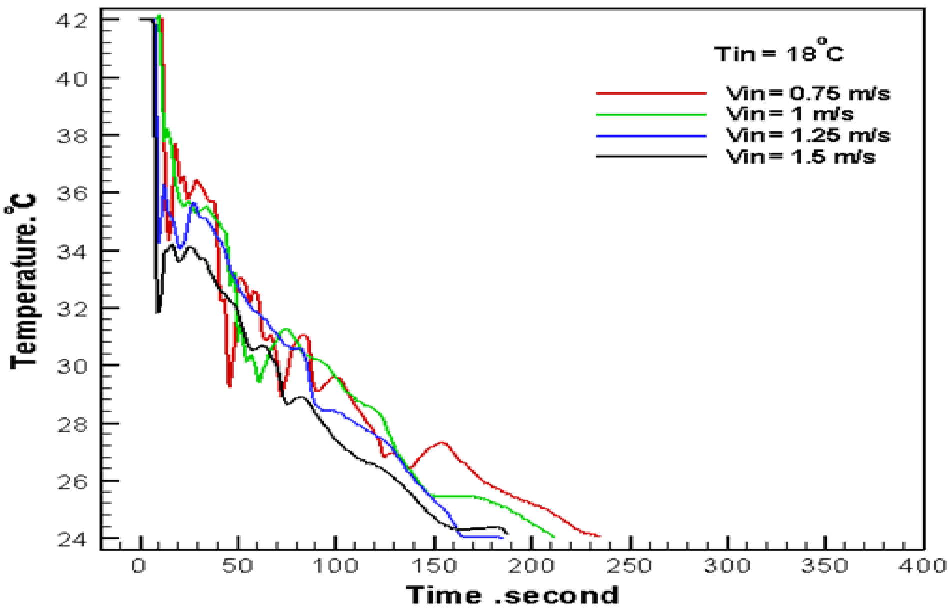

Figure 11. The relationship between the temperature of the room with time at inlet air temperatures (18^0C) and different-inlet air velocity in a displacement ventilation system and cooling ceiling.

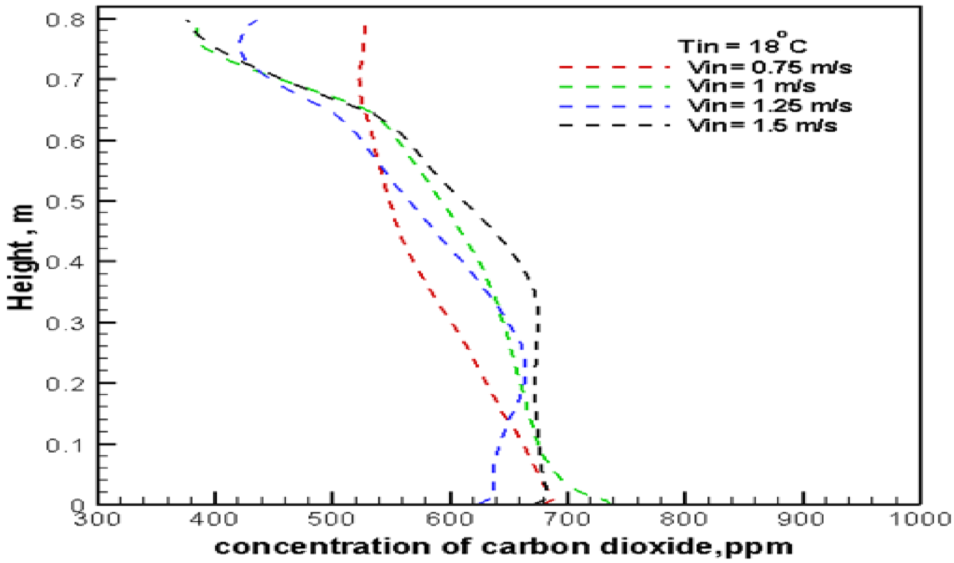

Figure 12. The relationship between the height of the room with co2 concentration inlet air temperature (18^{o}C) and different-inlet air velocity in a displacement ventilation and cooling ceiling system.

5. Conclusions

1. The experiments showed that thermal comfort was always achieved with ambient outdoor temperatures between (36 and 38^{o}C) with air inlet velocity of 0.7m/s and inlet temperature of 24^{o}C, for all of the considered mean penal temperatures (15, 16 and 17^{o}C). For the experimental FC case with T_{mp}=15^{o}C, comfort was achieved almost in all cases.
2. The effect of air inlet velocity was very significant when the air inlet temperature decreases from 24^{o}C to 20^{o}C and the results showed that the best case of the present work was when T_{ai}=20^{o}C and u_a=2m/s, while the other ordinary air-conditioning application supplies the air with lower temperature and higher velocity which means a bigger and chiller fan thus a higher cost as well.
3. With the introduction of mechanically induced FC, the corrugated ceiling RCP capacity increases by 8~13%, compared to still air, for discharge velocity of 2m/s when the room-to-metal sheet surface temperature differentials range from 5~12 °C.

Energy consumption is one of the most important factors considered in the selection of an HVAC system. The power saving capacity of the combined device includes:

a) The temperature of chilled water needed by the combined system by the disengagement of dehumidification from cooling is greater than that required by the traditional system. Higher water source temperature means higher chiller efficiency (COP). In addition, higher chilled water temperatures allow low energy or free cooling as an alternative to mechanical cooling.
b) The airflow supply decreases and so does the fan energy consumption, due to the decoupling of the ventilation heat transfer mechanisms.
c) A two-stage heat recovery exhaust air is used and cooling power is decreased.
d) Reheating of the air supply is not required as overcooling of the air is prevented.
e) Since the mean room temperature of the radiant CC system is lower than that of the conventional air conditioning system, for the same thermal comfort, the indoor air temperature may be higher than the traditional system and therefore energy saving may be achieved.

Nomenclature

D	Diameter	m
H	Height	m
h	Heat transfer coefficient	$W/m^2.K$
K	Turbulent Kinetic energy	---
k	Thermal conductivity	W/m.K
l	Scale Factor	---
L	Length	m
Q_{cap}	Corrugated ceiling RCP Capacity	W/m^2
S_{bj}	Buoyancy source or sink term	---
S_T	Source term in energy equation	---
T	Temperature	^oC
u, v, w	Stream-wise, lateral and vertical velocity components respectively	m/s
W	Width	m
w	Distance between the tubes	m
x, y, z	The corresponding Cartesian axis	---
Greek Symbols		
ε	Turbulent energy dissipation rate	---
δ	Thickness	mm
Γ	Diffusion coefficient	---
ΔT	Temperature difference	^oC
Subscripts		
a	air , space	
C	convection	
c	ceiling , characteristic	
eff.	Effective value	
f	fluid	
i	inside , inlet	
i, j, k	The three coordinate directions	
m	model , mean	
o	outside , outlet	
p	prototype , panel	
r	radiation	
t	per one tube	
w	water	
Abbreviations		
ACH	Air Change per Hour	
ASHRAE	American Society for Heating, Refrigeration, and Air Conditioning Engineering	
FC	Forced Convection	
MC	Mixed Convection	
NC	Natural Convection	
RCP	Radiant Cooling Panel	

6. References

[1] ASHRAE Handbook 2020 *HVAC Systems and Equipments (SI)* (Panel Heating and Cooling) Chapter 6
[2] T Moore, F Bauman and C Huizenga 2006 *Radiant Cooling Research Scoping Study* (Center for the Built Environment (CBE) University of California, Berkeley
[3] Corina Stetiu 1998 *Radiant Cooling in US Office Buildings: Towards Eliminating the Perception of Climate-Imposed Barriers* (Ph.D. Thesis, University of California at Berkeley)
[4] ASHRAE Standard 2016 *Ventilation for Acceptable Indoor Air Quality*

[5] ASHRAE Handbook 2017 *Fundamentals (SI)* (Pipe Sizing) Chapter 22
[6] The Copper Tubes Handbook 2010 *Copper Development Association*
[7] Nassir Ibraheem Khalaf 2008 *Experimental and Numerical Analysis of Air Outlet Configuration in Air-Conditioned Space* (M.Sc. Thesis, Technical College/Baghdad)
[8] Jae-Weon Jeong and Stanley A. Mumma 2003 *Impact of Mixed Convection on Ceiling Radiant Cooling Panel Capacity* (HVAC & R Research) vol 9 no 3 pp 251-256
[9] Jae-Weon Jeong and Stanley A Mumma *2004 Simplified Cooling Capacity Estimation Model for Top Insulated Metal Ceiling Radiant Cooling Panels* (Applied Thermal Engineering) vol 24 pp 2055-2072